Novel agarose polymer electrolyte for quasi-solid state dye-sensitized solar cell

Ying Yang[a,*], Hao Hu[b], Cong-Hua Zhou[c], Sheng Xu[b], Bobby Sebo[b], Xing-Zhong Zhao[b,**]

[a] School of Metallurgical Science and Engineering, Central South University, Changsha 410083, China
[b] Department of Physics and Key Laboratory of Artificial Micro- and Nano-structures of Ministry of Education, Wuhan University, Wuhan 430072, China
[c] School of Physical Science and Technology, Central South University, Changsha 410083, China

ARTICLE INFO

ABSTRACT

Quasi-solid state dye-sensitized solar cells (DSSCs) are fabricated with a novel polysaccharide gel electrolyte composed of agarose in 1-methyl-2-pyrrolidinone (NMP) as polymer matrix, lithium iodide (LiI)/iodine (I_2) as redox couple and titania nanoparticles as fillers. The polysaccharide electrolyte with different agarose concentrations (1–5 wt%) and various inorganic filler TiO_2 concentrations (0–10 wt%) are studied systematically by differential scanning calorimetry (DSC) and the AC impedance spectra. The electrochemical and photoelectric performances of DSSCs with these electrolytes are also investigated. It is found that increasing agarose and inorganic filler concentration leads to a decrease in T_g in the range of 1–2 wt% for agarose and 0–2.5 wt% for TiO_2 changed electrolytes, which results in high conductivity in these electrolytes. From the electrochemical analysis, it is observed that the electron lifetime in TiO_2 of DSSCs increases with agarose, while decreases with inorganic filler contents. The prolonged electron lifetime in DSSCs is advantageous to improve open-circuit voltage (V_{oc}). Based on these results, the cell with the electrolyte of 2 wt% agarose shows the optimized energy conversion efficiency of 4.14%. The optimized efficiency of the DSSC with added titania is 4.74% at 2.5 wt% titania concentration.

1. Introduction

Dye-sensitized solar cells (DSSCs) have been attracting intensive interest for scientific research and industrial applications because of their high photon-to-electricity conversion efficiency and low cost [1,2]. However, it is a challenge to use them outdoors due to their hard hermetic sealing requirements. Much effort has been directed to developing nonvolatile electrolytes meeting the stability requirements for outdoor applications [3–5]. One strategy attracting particular interest is to replace the liquid electrolyte with polymer gel [6] or solid electrolyte [7,8].

Due to the absence of solvent in the solid electrolyte, there are several serious problems existing, such as crystallization of the iodide salt, low ionic conductivity and poor ability to penetrate into the nanocrystalline TiO_2 films, all of which consequently deteriorate the cell performance and stability [9]. However, quasi-solid state polymer gel electrolyte has as high ionic conductivity as liquid electrolyte and also suppresses the solvent leakage, thus showing good stability.

Recent researches on polymer gel electrolyte proved that the incorporation of inorganic nanoparticle filler in polymer electrolyte yields higher ionic conductivity [10]. The filler provides a solid like support matrix, allowing the amorphous polymer to maintain its liquid-like characteristics in terms of fast ionic mobility at the microscopic level. This could help in enhancing the cell performance, and further could increase the stability and lifetime of these devices [11].

Polysaccharide, such as agarose and κ-carrageenan is considered to be good and environment-friendly polymer matrix for forming cross-linking networks with other components in the polymer electrolyte because of their rich hydroxyl groups in molecule structure. Meanwhile, polysaccharide shows much lower crystallinity at room temperature compared to traditional PEO matrix. These may lead to high ionic conductivity, and excellent thermal and chemical stability of polysaccharide electrolyte [12–14], making it suitable for use as heterogeneous medium in photoenergy conversion [15–17]. Although excellent achievements have been reached in studying polysaccharide electrolyte, until now there are seldom studies which make systematic reporting on the ionic or electronic transport process in DSSCs with polysaccharide electrolyte. On the other hand, few attempts have been made to investigate quasi-solid-state electrolytes prepared from agarose directly dissolved in organic solvents. This is because solubility of polysaccharides in an organic solvent is generally much lower than that in water as we generally know. Herein, the electrochemical and photovoltaic performances of agarose electrolyte based DSSCs with different agarose and inorganic filler TiO_2 concentrations are systematically studied. Also, a simple method
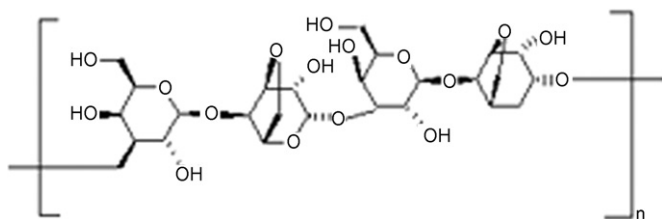
Fig. 1. Structure of agarose.

of preparing homogeneous agarose electrolyte was developed by directly dissolving agarose into 1-methyl-2-pyrrolidinone (NMP).

2. Experimental

2.1. Sample preparation

Agarose (commercial electrophoresis used, $M_w = 5000\,g\,mol^{-1}$) was purchased from SCRC in China and the molecular structure of the agarose in this study is presented in Fig. 1. Lithium iodide (LiI, 99%) was purchased from Acros. TiO_2 (P25, 20–30 nm) was purchased from Degussa AG, Germany. Iodine (I_2) and other common reagents were purchased from SCRC, China.

Agarose as host polymer, lithium iodide/iodine (LiI/I_2) as redox couple, 1-methyl-2-pyrrolidinone (NMP) as solvent and inorganic nanoparticle TiO_2 as filler were used to prepare the polymer electrolyte. To prepare the agarose electrolyte, firstly, different amounts of agarose (0.1–0.5 g) were added into 10 g NMP and these polymer solutions were stirred at 80 °C in the hermetic brown flask in silicone bath for 4 h. Then the inorganic nanoparticles (TiO_2, P25) with the concentration range 0–10 wt% of the agarose were slowly introduced and stirred for another 2 h. When preparing the electrolyte with various agarose concentrations, the inorganic filler TiO_2 content was fixed arbitrarily at 7.5 wt%. After optimization of TiO_2 content in electrolyte, the agarose content that was chosen for the filler TiO_2 variation was fixed at the optimized concentration of 2 wt% in which the corresponding DSSC obtained the best energy conversion efficiency. After that, solid LiI, and I_2 with $LiI/I_2 = 10:1$ (molar ratio, LiI: 0.08143 g; I_2: 0.01542 g) were added to the above polymer solutions at ambient environment. The polymer solution was stirred continuously in the hermetic brown flask until a homogeneous viscous liquid was formed.

Nanoporous TiO_2 electrodes were prepared according to previous report [18]. Assembly of the dye-sensitized solar cell was according to the following steps. The agarose electrolyte solution was dripped onto the dyed TiO_2 film. Then the electrolyte was heated under 73 °C to control the evaporation of the solvent in oven until it formed a very viscous gel. Finally, a sandwich-type DSSC configuration was fabricated by holding the platinum plate counter electrode together with the TiO_2/electrolyte with two clips. All the cells that based on agarose polymer electrolytes were assembled in the oven at 73 °C to avoid humidity.

2.2. Sample characterization

Differential scanning calorimetry (DSC) of the polymer electrolytes with different agarose and inorganic filler TiO_2 concentrations was carried out with Netzsch DSC 200PC (Germany). The samples were heated at a rate of 10 °C min^{-1} under nitrogen flow from −100 to 200 °C for DSC measurement. Approximately 5–7 mg of each sample was weighed and sealed in an aluminum pan for DSC analysis.

The ionic conductivity of polymer electrolytes was obtained using an electrochemical cell consisting of the electrolyte film sand-wiched between two platinum blocking electrodes. The impedance measurements of the electrolyte films were carried out on AC impedance analyzer (Agilent 4294A, USA) from 40 Hz to 1 MHz with signal amplitude of 10 mV. The ionic conductivity σ of the membrane is calculated by the following equation:

$$\sigma = \frac{L}{AR_b} \tag{1}$$

Here L is the thickness of the polymer electrolyte membrane and A is the area of the electrode. R_b is the bulk resistance of the gel electrolyte obtained from complex impedance measurements. The resistance (R_b) is taken at the intercept of the Nyquist plot with the real axis.

Electrochemical impedance measurements of the cells that based on these polymer electrolytes with different amounts of agarose and inorganic filler were also performed. The electrochemical impedance measurements were carried out on the CHI 660C electrochemical system (Chenhua, Shanghai), over the frequency range of 0.001–10^5 Hz and the perturbation voltage of 10 mV. These DSSCs were kept under illumination and a forward bias of −0.6 V was applied on all the samples.

Photocurrent–voltage (I–V) measurements were recorded by a two-electrode system under AM 1.5 illumination using Keithley Model 2400 Digital Source Meter unit (USA) by illuminating the cell through the active photoelectrode under a solar simulator (Oriel, 91192). The intensity of the incident light was calibrated by a Si-1787 photodiode (spectral response range: 320–730 nm). The incident power of the solar simulator was 73 mW cm^{-2}. The active DSSC area was controlled at 0.25 cm^2 by a mask. All of the measurements mentioned above were taken at ambient environment.

3. Results and discussion

3.1. DSC characteristics of electrolytes containing different agarose and inorganic filler contents

Differential scanning calorimetry (DSC) is usually used to investigate the phase transition of the polymer electrolytes. The glass transition temperature (T_g) is one of the most important parameters to illustrate the flexibility of the polymer at room temperature. Fig. 2 shows the change of T_g for the polymer electrolytes with different agarose and TiO_2 concentration. The glass transition appears in the heat flow curves as a step smeared over a certain range of temperatures. Here T_g is defined as the end temperature of the change in the heat flow curves occurs [19].

As seen in Fig. 2a, T_g firstly decreases as the agarose concentration increases from 1 wt% to 2 wt% and then increases when the agarose content exceeds 2 wt%. According to other studies [20–22], the decrease in T_g of electrolyte in the low polymer content range may be due to the interaction between the Lewis acid groups of salt (Li^+) and the surface hydroxyl of TiO_2 with the polar groups of agarose, which hinders the inter-molecule interactions within polymers. As a result, the mobility of the polymer chains increases and T_g decreases. The increase in T_g for the high polymer content (>2 wt%) may be due to the increased intermolecular interactions between agarose through hydrogen bonds.

Fig. 2b shows the relationship between the T_g and the filler TiO_2 nanoparticle contents (0, 2.5, 5, 7.5, 10 wt%) in the agarose electrolytes. The T_g values start from −77.3 °C when there is no filler added, then decreases gradually to −86.3 °C at 2.5 wt% TiO_2 content and finally increases continuously to −60.8 °C as the filler concentration increases to 10 wt%. When the added TiO_2 concentration increases from 0 to 2.5 wt%, the observed lower T_g value at 2.5 wt% is believed to be due to the interaction between the −OH groups in agarose and the filler TiO_2, which hinders the inter/intra-molecule cross-linking interactions within/between polymers [23]. Mean-
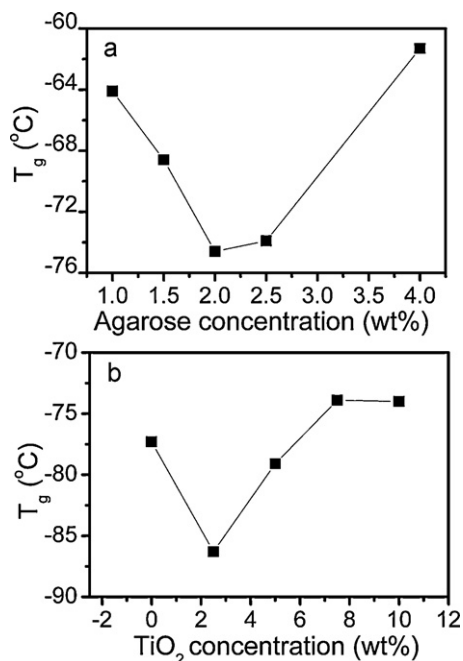
Fig. 2. Glass transition temperature, T_g, of agarose electrolytes depending on: (a) the agarose concentration; (b) the TiO_2 concentration.

while, the rapid increase in T_g in the high TiO_2 nanoparticle content (≥ 5 wt%) is due to the possible formation of crystalline phase when the abundant filler particles act as the nucleation centers of the crystalline polymer phase [24].

3.2. The influence of agarose and TiO_2 content on the conductivity of the agarose electrolyte

Table 1 shows the conductivity of the polymer electrolytes with varied agarose contents (1–4 wt%) and TiO_2 contents (0–10 wt%). It is observed that the ionic conductivity increases with agarose content up to 1.5 wt% and then decreases as the agarose content is further increased. The highest ionic conductivity at room temperature (30 °C) is found to be 3.94×10^{-4} S cm^{-1} for 1.5 wt% of agarose content.

At low agarose concentrations (1–1.5 wt%), the initial increase in the ionic conductivity is attributed to the low T_g of the polymer electrolyte and the increase in free ion concentration with the dissociation of LiI through the complex interaction between the hydroxyl in agarose with the Li$^+$ [25]. At higher agarose concentrations (>1.5 wt%), the increased polymer content hinders ionic movement and increases the viscosity of the electrolytes, thus reduces the ionic conductivity [26].

As for the agarose electrolytes with varied TiO_2 contents (Table 1), the ionic conductivity increases with TiO_2 content up to 5 wt%, reaching a maximum value of 5.12×10^{-4} S cm^{-1}, and then

Table 1
The conductivity of the DSSCs using the agarose electrolytes with different agarose and titania concentrations (wt%).

Agarose in electrolyte (wt%)	σ ($\times 10^{-4}$ S cm^{-1})	TiO_2 in agarose (wt%)	σ ($\times 10^{-4}$ S cm^{-1})
1	2.80612	0	2.97619
1.5	3.94406	2.5	4.40141
2	3.64538	5	5.10204
2.5	3.21709	7.5	3.33778
3	0.65206	10	3.40136
5	0.66153		
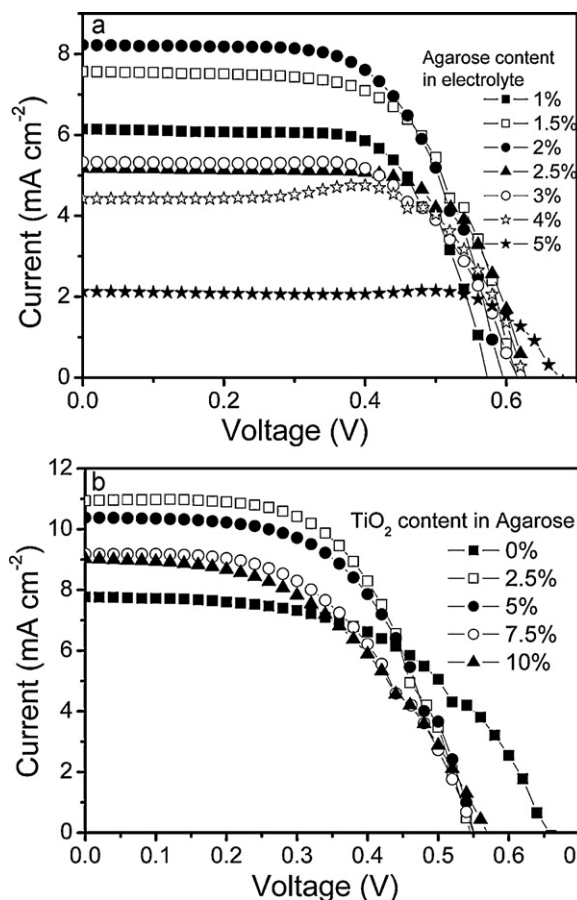
Fig. 3. Photocurrent–voltage curves of the DSSCs with agarose electrolytes: (a) with various agarose concentrations (wt%); (b) with various TiO_2 filler concentrations (wt%).

decreases as the filler increases to 10 wt%. At low TiO_2 contents (≤ 5 wt%), the enhancement of ionic conductivity in the electrolyte is related to the interaction between the hydroxyl groups in agarose and the surface hydroxyl groups on TiO_2 nanoparticles, which results in a continuous ion transport pass way in the electrolytes, thus increases the ionic conductivity. However, at high TiO_2 contents (>5 wt%), the decrease in conductivity is believed to be due to the formation of continuous non-conductive phase by the excess ceramic fillers, which blocks the ion transport in the electrolytes, leading to low ionic conductivity [27].

3.3. Photovoltaic performance of the agarose electrolyte based DSSCs with various agarose and inorganic filler contents

The photovoltaic characteristics of the DSSCs obtained by incorporating different agarose concentrations (1–5 wt%) and inorganic filler (TiO_2) contents (0–10 wt%) under a constant illumination intensity of 73 mW cm^{-2} (AM 1.5) are shown in Fig. 3. The dependence of short-circuit current (J_{sc}), open-circuit voltage (V_{oc}), the fill factor (FF), and the photo-to-electric conversion efficiency (η) on the agarose and TiO_2 concentration are shown in Table 2.

As for the DSSCs with various agarose contents shown in Table 2, it is seen that J_{sc} and the conversion efficiency (η) of the DSSCs increase with agarose concentration until a maximum value is reached at the polymer concentration of 2 wt%, after which further increase of agarose to 5 wt% causes a drop in J_{sc} and η. The open-circuit photovoltage (V_{oc}) increases with agarose content in

Table 2
The parameters obtained from the photocurrent–voltage (I–V) curves of the DSSCs using the agarose-based polymer electrolyte measured under a constant illumination intensity of 73 mW cm^{-2} (AM 1.5).

Content (wt%)	J_{sc} (mA cm^{-2})	V_{oc} (V)	FF	η (%)
Agarose (in electrolyte)				
1	6.16	0.575	0.672	3.2
1.5	7.56	0.617	0.632	3.97
2	8.24	0.597	0.625	4.14
2.5	5.16	0.625	0.693	3.01
3	5.32	0.618	0.639	2.83
4	4.44	0.630	0.724	2.73
5	2.12	0.675	0.775	1.49
TiO$_2$ (in agarose)				
0	7.76	0.660	0.528	3.77
2.5	10.96	0.545	0.570	4.74
5	8.84	0.550	0.559	4.45
7.5	9.20	0.550	0.516	3.64
10	9.04	0.570	0.476	3.42

the whole content range studied. The best efficiency (η) of 4.14% is reached at 2 wt% agarose electrolyte based DSSC.

For the DSSCs based on different agarose concentrations, the V_{oc} increases significantly from 0.575 to 0.675 V as the concentration of agarose increases from 1 to 5 wt%, corresponding to a voltage shift of 100 mV (Table 2). According to the theoretical study conducted by Huang et al. [28], the change of V_{oc} in DSSCs is related to the electron content change in the anode TiO$_2$. It is known that the accumulated electrons in TiO$_2$ are originated from the electron injection of the excited dye molecules to the conduction band of TiO$_2$. In the low agarose content range (1–2 wt%), the introduction of a small amount of polymer into the electrolyte improves the dissociation of LiI, resulting in an increase in I$^-$/I$_3^-$ content in the electrolyte and an improvement in ionic conductivity (Table 1). With the increase of I$^-$ ions in the electrolytes, the regeneration of the oxidized dye is expected to be accelerated and the accumulated electrons in TiO$_2$ via charge injection from excited dye molecules increase, resulting in a higher V_{oc}. As the agarose content increases exceeding 2 wt%, because the agarose contain many hydroxyl groups in its molecule, it is easy for agarose to form a cross-linking interaction with TiO$_2$ through hydrogen bonds. This effect hinders the charge recombination between the I$_3^-$ in electrolyte with the electrons in conduction band of TiO$_2$, thus improving the V_{oc}. So, in the whole agarose content studied the V_{oc} increases with agarose content.

As seen in Table 2, the J_{sc} of the DSSCs with different TiO$_2$ contents increases appreciably from 7.76 to 11 mA cm^{-2} when TiO$_2$ content increases from 0 to 2.5 wt% and then decreases as TiO$_2$ content further increases. While the V_{oc} decreases with increasing TiO$_2$ concentration from 0 to 10 wt%. The best efficiency (η) of 4.74% is obtained at 2.5 wt% TiO$_2$ contained DSSC.

For the DSSCs based on different TiO$_2$ contents, the V_{oc} decreases from 0.66 to 0.57 V as the concentration of titania increases from 1 to 10 wt% (Table 2). Because the interaction between the LiI and the surface –OH groups in TiO$_2$ will increase with TiO$_2$ content in polymer electrolyte, the dissociation of LiI will increase. This effect increases the Li$^+$ content in the electrolytes. Lithium ions are subject to adsorb on the surface of the added TiO$_2$, which makes the added TiO$_2$ accumulated of positive charges. According to the same considerations [28] discussed above on V_{oc}, once the electrolyte drops onto the dyed anode, the positive charged added-TiO$_2$ contacts with the anode TiO$_2$, which decreases the electron content in the anode and the V_{oc} of DSSCs decreases [29,30]. Chatzivasiloglou et al. [31] reported a similar result that the V_{oc} of the DSSCs decreases with the content of TiO$_2$ added in PEO electrolyte, which is believed to be due to the adsorption of Li$^+$ onto the surface of TiO$_2$.

3.4. Electrochemical characterization of the agarose electrolyte based DSSCs with different agarose and TiO$_2$ nanoparticle concentrations

Electrochemical impedance spectroscopy (EIS) is a powerful technique for characterization of electronic or ionic transport process in DSSCs [32–35]. To further understand the electronic transport process that influences the J_{sc} and V_{oc} of DSSCs with varied agarose and TiO$_2$ contents in electrolyte, the electrochemical impedance spectra of the cells with these two series of polymer electrolytes were measured under illumination of 73 mW cm^{-2} as shown in Fig. 4. The figures are given in the form of Nyquist (Fig. 4a) and Bode (Fig. 4b and c) plots, respectively.
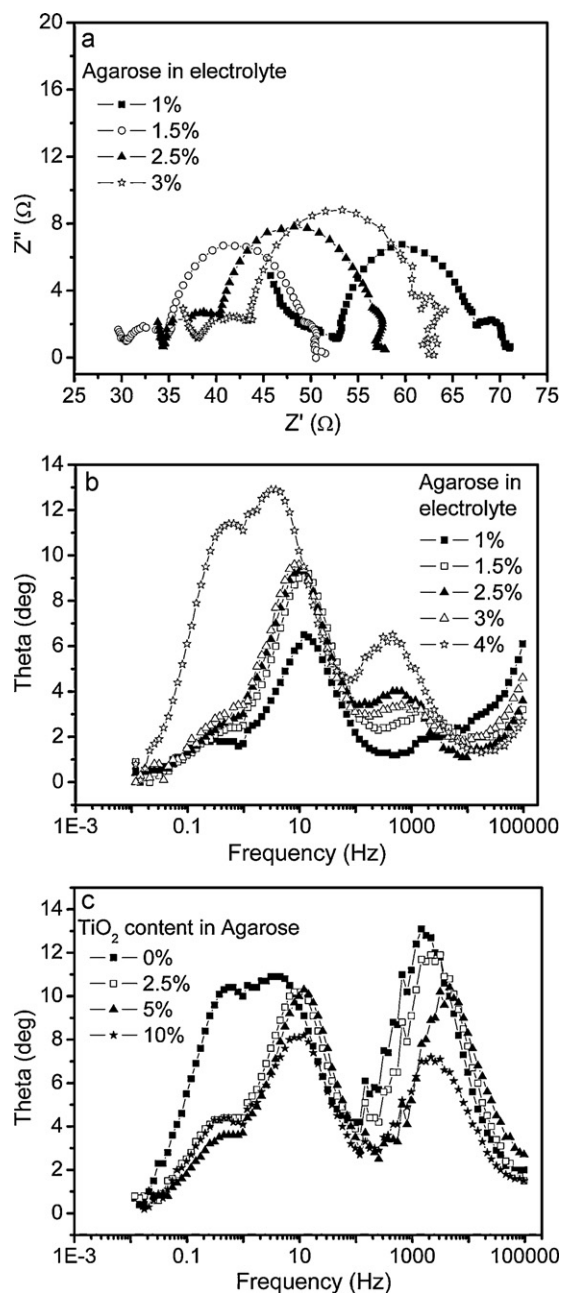
Fig. 4. Electrochemical impedance spectrum (EIS) of the DSSCs based on agarose electrolytes: (a) Nyquist plots of DSSCs with different agarose concentrations; (b) the Bode phase plots of DSSCs with different agarose concentrations; (c) the Bode phase plots of DSSCs with different TiO$_2$ concentrations.

Table 3
The internal resistance elements (R_1 and R_2) measured from the three semicircles (Z_1 and Z_2); and the electron life time (τ) in TiO_2 anode measured from the characteristic middle frequency range in Bode plots of the electrochemical impedance spectra shown in Fig. 4.

wt%	R_1 (Ω)	R_2 (Ω)	Characteristic middle frequency (Hz)	τ (s)
Agarose (in electrolyte)				
1	–	14.6	13.10	0.07634
1.5	4.3	14.5	12.00	0.08333
2.5	6.5	15.6	10.07	0.0993
3	5.5	17.5	8.43	0.11862
4	8.1	33.6	3.47	0.28818
TiO_2 (in agarose)				
0	12.0	20.9	4.16	0.24038
2.5	9.8	10.3	9.66	0.10352
5	9.1	11.1	11.50	0.08696
10	7.5	8.9	9.66	0.10352

There are three peaks in Bode phase plots and three semicircles in the Nyquist plots which are attributed to the charge-transfer processes ($I_3^- + e = 3I^-$) at the Pt/electrolyte interface (Z_1, frequency range 10^3–10^5 Hz); the charge recombination reaction process ($I_3^- + 2e_{cb}^-(TiO_2) = 3I^-$) occurring at nanocrystalline TiO_2/electrolyte interface (Z_2, frequency range 1–10^3 Hz); and the I^-/I_3^- diffusion process occurring in the electrolyte (Z_3, frequency range 10^{-1}–1 Hz) [36,37]. The parameters of R_1 and R_2 characterize the charge transfer resistance at Pt/electrolyte interface and the charge recombination resistance at nanocrystalline TiO_2/electrolyte interface, respectively.

Table 3 shows the charge transfer resistance at the Pt/electrolyte interface (R_1), the charge recombination resistance (R_2) at nanocrystalline TiO_2/electrolyte interface, the characteristic middle frequencies in Bode plots and the electron life time (τ) in TiO_2 of the DSSCs with varied agarose and TiO_2 concentrations in electrolyte. In the Bode phase plots, the characteristic middle frequencies are inversely proportional to the electron lifetime ($\omega = \tau^{-1}$) in TiO_2 according to the EIS theory [38,39].

Both R_1 and R_2 of the DSSCs increase with agarose concentration from 1 to 5 wt%. According to Wang's study [37], the increased value of R_1 implies that the reduction of triiodide at the Pt/electrolyte interface ($I_3^- + e = 3I^-$) is hindered in the DSSCs, usually leading to the decrease in J_{sc}. However, from Table 2, the J_{sc} values of DSSCs with different agarose contents follow an increase–decrease trend in the whole agarose content studied. Evaluation from both the ionic conductivity and EIS studies, the increase of J_{sc} in the low agarose concentration ($\leq$2 wt%) is attributed to the relatively high ionic conductivity as seen in Table 1. The decrease of J_{sc} in the high agarose concentration (>2 wt%) may be due to the increase in viscosity of the polymer electrolytes, which hinders the ion transport in the electrolyte, resulting in both increased R_1 in DSSCs and decreased ionic conductivity in high agarose contained electrolyte, leading to low J_{sc}.

R_2 increases with the agarose concentrations, indicating that the suppression of the charge recombination reaction between TiO_2 conduction band electrons and triiodide ions ($I_3^- + 2ecb^-(TiO_2) = 3I^-$) is more effective at higher agarose content electrolyte, resulting in the improvement of V_{oc} [37]. As seen in Table 3, the characteristic middle frequency of DSSCs moves to lower frequency with increasing agarose content in the electrolyte. The middle frequency peak, which is located at 12.08 Hz of the 1 wt% agarose electrolyte, moves gradually to 3.53 Hz as the agarose content increases to 4 wt%. The electron lifetime (τ) within the nanocrystalline TiO_2/electrolyte increases with agarose content, which indicates a prolonged electron lifetime and less back-reaction in the higher polymer content based DSSCs. The reduced electron back-recombination augments the quasi-Fermi

level of the conduction band electrons in the TiO_2 film and that may improve V_{oc} [40,41]. These results further confirm the conclusion that the V_{oc} increases with agarose content as shown in Table 2.

As for the DSSCs with different TiO_2 content, both R_1 and R_2 of the DSSCs decrease with TiO_2 concentration in the range of 0–10 wt%, which is contrary to that of agarose changed DSSCs. The decreased value of R_1 indicates that the charge transport resistance of the interface of Pt/polymer electrolyte is reduced, which accelerates the reduction of triiodide at the counter-electrode ($I_3^- + e = 3I^-$), leading to an increase in J_{sc} [37]. While in our studies, an increase–decrease trend of J_{sc} values was observed as the TiO_2 content increases in the DSSCs (Table 2). Similarly, considering both conductivity and EIS tests, the increase of J_{sc} in the low TiO_2 content range (0–2.5 wt%) results from both decreased R_1 in DSSCs and increased ionic conductivity in the electrolyte; and the decreased J_{sc} in the TiO_2 contents exceeding 2.5 wt% is mainly due to the formation of continuous non-conductive phase by the excess TiO_2, which block the ion transport in the electrolytes, leading to low J_{sc}.

R_2 decreases with TiO_2 concentration, indicating that the charge recombination in the electrolyte/TiO_2 interface increases, resulting in a decrease in V_{oc}. From Table 3, the characteristic middle frequency peaks of the DSSCs shifts from 3.98 Hz to 11.5 Hz as TiO_2 contents increases from 0 to 10 wt%. The calculated electron lifetime (τ) at the nanocrystalline TiO_2/electrolyte interface decreases with the increase in TiO_2 content, which indicates a shorter electron lifetime and more back-reaction in the higher TiO_2 content based DSSCs. The increased electron back-recombination implies lower V_{oc} of the DSSCs. These results also confirm the conclusion that the V_{oc} decreases with TiO_2 content shown in Table 2.

4. Conclusions

Agarose electrolytes for DSSCs with different polymer and inorganic filler TiO_2 concentrations were studied systematically by DSC, AC impedance spectra, photovoltaic studies and electrochemical analysis. The initial increase in both agarose and TiO_2 concentrations improves the conductivity of the polymer electrolytes, while further increase in both concentrations makes the conductivity decrease. Optimization of the electrolyte composition, such as agarose and inorganic filler TiO_2 concentration, is necessary to improve the energy conversion efficiency of the DSSCs. The maximum energy conversion efficiency of 4.74% was achieved at 2 wt% agarose and 2.5 wt% TiO_2 filler in the polymer electrolyte. The V_{oc} of the cells with these polymer electrolytes increases with agarose concentration, while it decreases with TiO_2 concentration in electrolyte. This result is closely related to the electron lifetime in the TiO_2 photoelectrode of cells according to electrochemical impedance studies.

Acknowledgments

References

[1] B. O'Regan, M. Grätzel, Nature 353 (1991) 737.
[2] M. Grätzel, Nature 414 (2001) 338.
[3] A.F. Noguei, C. Longo, M.A. De Paoli, Coord. Chem. Rev. 248 (2004) 1455.
[4] Y. Bai, Y.M. Cao, J. Zhang, M.K. Wang, R.Z. Li, P. Wang, S.M. Zakeeruddin, M. Grätzel, Nat. Mater. 7 (2008) 626.

[5] S. Cerneaux, S.M. Zakeeruddin, J.M. Pringle, Y.B. Cheng, M. Grätzel, L. Spiccia, Adv. Funct. Mater. 17 (2007) 3200.
[6] J.H. Wu, S.C. Hao, Z. Lan, J.M. Lin, M.L. Huang, Y.F. Huang, L.Q. Fang, S. Yin, T. Sato, Adv. Funct. Mater. 17 (2007) 2645.
[7] J.H. Wu, S.C. Hao, Z. Lan, J.M. Lin, M.L. Huang, Y.F. Huang, P.J. Li, S. Yin, T. Sato, J. Am. Chem. Soc. 130 (2008) 11568.
[8] P. Wang, S.M. Zakeeruddin, J.E. Moser, M.K. Nazeeruddin, T. Sejugychi, M. Grätzel, Nat. Mater. 2 (2003) 402.
[9] D. Saikia, C.C. Han, Y.W. Chen-Yang, J. Power Sources 185 (2008) 570.
[10] F. Croce, G.B. Appetecchi, L. Persi, B. Scrosati, Nature 394 (1998) 456.
[11] H.W. Han, W. Liu, J. Zhang, X.-Z. Zhao, Adv. Funct. Mater. 15 (2005) 1940.
[12] M. Kaneko, N. Mochizuki, K. Suzuki, H. Shiroishi, K. Ishikawa, Chem. Lett. 5 (2002) 530.
[13] H. Ueno, M.J. Kaneko, Electroanal. Chem. 568 (2004) 87.
[14] H. Ueno, Y. Endo, Y. Kaburagi, M.J. Kaneko, Electroanal. Chem. 570 (2004) 95.
[15] M. Kaneko, T. Hoshi, Chem. Lett. 32 (2003) 872.
[16] M. Kaneko, T. Hoshi, Y. Kaburagi, H. Ueno, Electroanal. Chem. 572 (2004) 21.
[17] K. Suzuki, M. Yamaguchi, M. Kumagai, N. Tanabe, S. Yanagida, C. R. Chimie 9 (2006) 611.
[18] Y. Yang, C.H. Zhou, S. Xu, H. Hu, B.L. Chen, J. Zhang, S.J. Wu, W. Liu, X.Z. Zhao, J. Power Sources 185 (2008) 1492.
[19] D. Bamford, A. Reiche, G. Dlubek, F. Alloin, J.Y. Sanchez, M.A. Alam, J. Chem. Phys. 118 (2003) 9420.
[20] C. Becker, H. Krug, H. Schmidt, Mater. Res. Soc. Symp. Proc. 435 (1996) 237.
[21] W. Hergeth, U. Steinau, H. Bittrich, G. Simon, K. Schmutzler, Polymer 30 (1989) 254.
[22] K. Iisaka, K. Shibayama, J. Appl. Polym. Sci. 22 (1978) 3135.
[23] B.J. Ash, L.S. Schadler, R.W. Siegel, Mater. Lett. 55 (2002) 83.
[24] B.K. Choi, Y.W. Kim, K.H. Shin, J. Power Sources 68 (1997) 357.
[25] J.P. Sharma, S.S. Sekhon, Solid State Ionics 178 (2007) 439.
[26] W. Li, J. Kang, X. Li, S. Fang, Y. Lin, G. Wang, X. Xiao, J. Photochem. Photobiol. A 170 (2005) 1.
[27] Z.Y. Wen, T. Itoh, M. Ikeda, N. Hirata, M. Kubo, O. Yamamoto, J. Power Sources 90 (2000) 20.
[28] S.Y. Huang, G. Schlichthor, A.J. Nozik, M. Grätzel, A.J. Frank, J. Phys. Chem. B 101 (1997) 2576.
[29] D. Kuang, C. Klein, H.J. Snaith, J.E. Moser, R. Humphry-Baker, P. Comte, S.M. Zakeeruddin, M. Grätzel, Nano Lett. 6 (2006) 769.
[30] S. Nakade, T. Kanzaki, W. Kubo, T. Kitamura, Y. Wada, S. Yanagida, J. Phys. Chem. B 109 (2005) 480.
[31] E. Chatzivasiloglou, T. Stergiopoulos, A.G. Kontos, N. Alexis, M. Prodromidis, P. Falaras, J. Photochem. Photobiol. A 192 (2007) 49.
[32] D. Kuang, S. Ito, B. Wenger, C. Klein, J.E. Moser, R. Humphry-Baker, S.M. Zakeerudddin, M. Grätzel, J. Am. Chem. Soc. 128 (2006) 4146.
[33] D. Kuang, P. Wang, S. Ito, S.M. Zakeeruddin, M. Grätzel, J. Am. Chem. Soc. 128 (2006) 7732.
[34] J. Bisquert, J. Phys. Chem. B 106 (2002) 325.
[35] J. Bisquert, A. Zaban, M. Greenshtein, I. Mora-Sero, J. Am. Chem. Soc. 126 (2004) 13550.
[36] N. Fuke, A. Fukui, R. Komiya, A. Islam, Y. Chiba, R. Yanagida, R. Yamanaka, L. Han, Chem. Mater. 20 (2008) 4974.
[37] M. Wang, Y. Lin, X.W. Zhou, X.R. Xiao, L. Yang, S.J. Feng, X.P. Li, Mater. Chem. Phys. 107 (2008) 61.
[38] Q. Wang, J.E. Moser, M. Grätzel, J. Phys. Chem. B 104 (2005) 2044.
[39] R. Kern, R. Sastrawan, J. Ferber, R. Stangl, J. Luther, Electrochim. Acta 47 (2002) 4213.
[40] Z.P. Zhang, S.M. Zakeeruddin, B. O'Regan, R. Humphry-Baker, M. Grätzel, J. Phys. Chem. B 109 (2005) 21818.
[41] J.J. He, G. Benko, F. Korodi, T. Polivka, R. Lomoth, B. Akermark, L.C. Sun, A. Hagfeldt, V. Sundstrom, J. Am. Chem. Soc. 124 (2002) 4922.